Influence of near-surface strongly anisotropic medium on P-to-S wave conversion

Rina YONEKI[1], Hitoshi MIKADA[2], and Junichi TAKEKAWA[2]

[1]Dept. of Civil and Earth Res. Eng., Kyoto University (Now at East Japan Railway Company)
[2] Dept. of Civil and Earth Res. Eng., Kyoto University

Formations, like near surface and reservoir rock, are estimated to be strongly anisotropic for elastic wave propagation. To extract anisotropic information from seismic exploration data, many researches have conducted elastic anisotropy studies. However, most of these studies are based on the assumption of weakly anisotropic media. Our previous studies showed that strong anisotropic media in the subsurface significantly influence the seismic waveforms especially on the PS converted waves. In the present study, we apply the reverse time migration (RTM) to the PS converted waves to determine the depth of anisotropic layer. In addition, we normalized them and take difference for comparing imaging results. To extract PS converted waves from observed data, we also develop a novel wave separation method. We demonstrate the effectiveness of our method using a numerical experiment. Our numerical result shows that our method can image layer boundary between isotropic and anisotropic layers which generates PS converted waves.

1. INTRODUCTION

In the fields of earthquake disaster prevention and energy resource exploration, understanding the properties of seismic anisotropy is important for obtaining various information about subsurface, for example, its structure, regional stress field and selective orientation of crack opening direction. As studies of seismic velocity anisotropy, many researches have carried on about azimuthal anisotropy and S-wave splitting as fundamental researches for imaging of subsurface materials. Recent development of unconventional hydrocarbon reservoirs has revealed that subsurface materials, like shale rock and unconsolidated near surface sediments, are much anisotropic than expected[1)]. In association with increasing shale oil and gas exploration, demands for powerful geophysical exploration method for strongly anisotropic material are increasing. However, in most of those studies, the magnitude of anisotropy is assumed to be weak[2)]. In addition, there are few studies on seismic wavefields in quite strongly anisotropic media.

In our previous research, to obtain detailed information of near surface anisotropy, we investigated the influence of strong anisotropy on received seismic waveforms with numerical simulations using finite-difference method (FDM) [3)]. Our results showed that we could obtain information about subsurface anisotropy by focusing P-S converted wave which observed between direct P- and S-waves in waveforms.

In this study, taking the above into account, we build a hypothesis that we could identify the position of anisotropic material which affect received waveforms by use of P-S converted wave. We investigate how magnitude of anisotropy affects where P-S wave generates using the reverse time migration (RTM). RTM is one of the migration methods for imaging generating position of scattering wave which recorded in receiver positions. In our investigation, to implement RTM using recorded P-S wave, we use the two ways for extracting P-S wave from received waveforms; one is muting and the other is using P- and S-wave separation method that we develop. In the case of muting, we normalize imaging results of RTM and take difference between normalized imaging results of three models with different magnitude of anisotropy. By comparing normalized imaging results, we verify the relationship between magnitude of anisotropy and distribution of P-S wave generating points and capability of detecting subsurface anisotropy. In this paper, we show the numerical calculation method including the new wave separation method and RTM results.

2. NUMERICAL SIMULATION METHOD

(1) Reverse time migration

Reverse time migration (RTM) is now one of the widely used imaging method and provides high resolution images even for complicated geometries. For imaging, we correlate source wavefield from sources to scatter points and receiver wavefield from receivers to scatter points. Receiver wavefield can be obtained by back propagation calculation of received data. In our study, we use crosscorreation imaging condition (equation (1)) proposed by Claerbout (1971)[4].

$$I(x,y,z) = \int u_s(x,y,z,t)u_r(x,y,z,t)dt \qquad (1)$$

Note that, I is imaging result in location (x,y,z), u_s is source wavefield and u_r is receiver wavefield in location (x,y,z) and in time t.

(2) Wave separation method using displacement potentials

Vector wavefield can be decomposed into a scalar potential and a vector potential. This is known as Helmholtz's theorem. By applying this theorem to displacement vector, displacement wavefield **u** can be represented by one scalar potential ϕ and two vector potentials **A** and **B**,

$$\mathbf{u} = \nabla\phi + \nabla\times\mathbf{A} + \nabla\times(\nabla\times\mathbf{B}). \qquad (2)$$

When **A** and **B** are chosen as $\mathbf{A} = (0,0,\chi)$ and $\mathbf{B} = (0,0,\psi)$ and substituted to elastic wave equation, ϕ should satisfy scalar wave equation of compressional wave, χ and ψ should satisfy scalar wave equation of shear wave[5]. The three scalar potentials (ϕ, χ and ψ) are displacement potentials of P-wave, SH-wave and SV-wave, respectively. Using displacement potentials, wavefields of P-wave, SH-wave and SV-wave are can be calculated individually from received data of displacement recorded on the surface.

To calculate displacement potentials using equation (2), we approximate the equation (2) with $\mathbf{A} = (0,0,\chi)$ and $\mathbf{B} = (0,0,\psi)$ by difference formula. Then, we make a system of linear equation for ϕ, χ and ψ and solve it using received data of displacement in each time steps. Note that, to calculate partial derivative of vertical direction $\partial/\partial z$, we use three set of receivers; mid, upper and lower receivers (**Fig. 1**). Therefore, when we want to obtain displacement potentials in the mid receivers (suppose they are on the surface), we need received data of displacement of three sets of

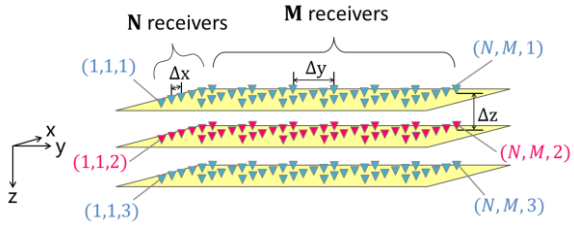

Figure 1 Receivers used for wave separation method using displacement potentials. Red colored receivers are mid receivers.

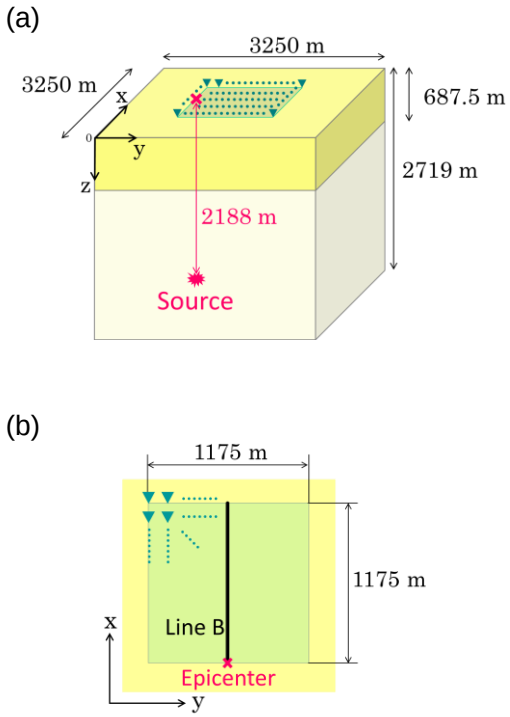

Figure 2 (a) Horizontally layered model and (b) receivers and position of line B.

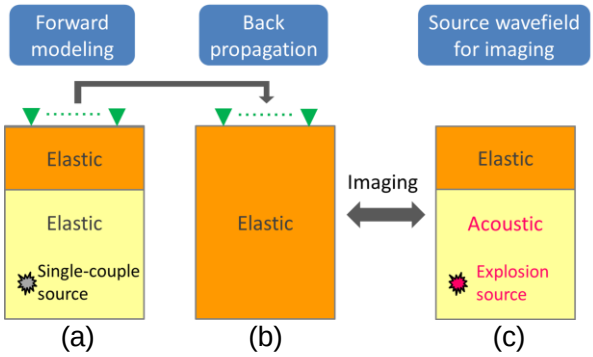

Figure 3 Numerical models for RTM. (a) is for forward modeling and data acquisition, (b) is for back propagation and receiver wavefield acquisition and (c) is for source wavefield acquisition.

receivers. Furthermore, because coefficient matrix of linear system is ill-conditioned, we use singular value decomposition (SVD) to solve the equation.

(3) Wave propagation calculation

The Governing equations are the equation of motion[6] and the constitutive relationship (Hook's low) that given as equations (3) and (4), respectively.

$$\rho\,\ddot{u}_i = \tau_{ij,j} + f_i\,, \tag{3}$$

$$\tau_{ij} = c_{ijkl}\varepsilon_{kl}\,. \tag{4}$$

In equation (3), u_i is particle displacement vector, $\tau_{ij,j}$ is stress tensor, f_j is body force that represents source and ρ is density. In equation (4), c_{ijkl} is stiffness tensor and ε_{kl} is strain tensor.

Property of anisotropic media can be defined by stiffness tensor c_{ijkl}. In this study, we use VTI medium (transversally isotropic media with a vertical axis of symmetry) as an anisotropic medium. VTI is one of typical anisotropic media and is isotropic in horizontal plane. Stiffness matrix of VTI can be written by five independent parameters.

To calculate elastic wave propagation, we use FDM with rotated staggered grid[7]. Rotated staggered grid scheme increases numerical error because components of velocity and stress components are defined in the same grid cell point, respectively, and there is no need to interpolate velocity and c_{ijkl}. So it can be applied to general anisotropic media including lower symmetry of anisotropy than orthorhombic.

3. FORWARD MODELING

To investigate how strong anisotropy affects the received wavefield and implement RTM, we conducted numerical experiments using three different inhomogeneous models. They are horizontally layered models with different magnitude of anisotropy for upper layers. These degrees of anisotropy are 30%, 10% and 0% (isotropic).

(1) Forward calculation model

Three horizontally layered models have different upper layers with the same structure (**Fig. 2(a)**). The top of models is the ground surface using free boundary condition. To express semi-infinite media, we implement CPML boundary[8] for other five faces. The one model has a VTI upper layer with degree of magnitude 30%. This means the ratio of the maximum velocity (horizontal direction) and the minimum velocity (vertical direction) is 30%. Other model has a VTI upper layer with degree of magnitude 10%. The other has an isotropic upper layer. We call these models as "30% VTI model", "10% VTI model" and "isotropic model". The stiffness coefficients of 30 % VTI model are C_{11}= 20.45 GPa, C_{33}= 12.10 GPa, C_{13}= 5.113 GPa, C_{44}= 4.900 GPa and C_{66}= 8.281 GPa. Those of 10 % VTI model are C_{11}= 14.64 GPa, C_{33}= 12.10 GPa, C_{13}= 3.127 GPa, C_{44}= 4.900 GPa and C_{66}= 5.929 GPa. Phase velocities of the isotropic model is Vp = 2200 m/s and Vs = 1400m/s, so vertical velocity of three upper media is the same as each other. The lower layers of three models are the same isotropic media with Vp = 2400 m/s and Vs = 1900m/s, The density of three models is the same 2500 kg/m^3.

The size of models is 3250m × 3250m × 2719m in x-, y- and z-directions. The source is located at x = 1094m, y = 1625m and z = 2188m. The type of the source and the function is Ricker wavelet with a dominant frequency of 12Hz and the excitation direction is vertical direction (z-direction). 9025 receivers are located in the area of square shape on the surface with interval 12.5m (**Fig. 2(b)**). Line B is in the center of square area along the x-direction.

(2) Back propagation model

To implement RTM, it is necessary to extract P-S wave in recorded data and to calculate back propagation. In P-S wave imaging, wave derived from shear wave source, like S-wave and S-P wave, is one of cause for noise in imaging result. Taking that into consideration, as source wavefield for RTM, we calculate wave propagation in acoustic media (Vs = 0m/s) that only P-wave is generates (**Fig. 3(c)**). By changing lower layer to acoustic media and the source type to explosion source, large amplitude of S-wave does not appear in wavefield, it would be effective for decreasing noise in P-S wave imaging. Also, for back propagation, we use homogeneous models with the same properties of upper media of 30% VTI model, 10% VTI model and isotropic model (**Fig. 3(b)**). It would decrease noise due to multiple reflections from the layer boundary.

4. IMAGING RESULTS

(1) Muting waveforms excluding P-S waves

In this section, we extract only P-S wave from received waveforms for RTM by muting received waveforms excluding P-S waves. **Fig. 4** shows received waveform of particle velocity in line B of 30% VTI model, 10% VTI model and isotropic

model. **Fig. 5** shows RTM imaging results of x-direction displacement in vertical planes just beneath line B of three models. In **Fig. 5**, we can see strong signals of boundaries around the depth 700m. This value almost conforms to the location of the layer boundaries (z = 687.5m).

Next, we normalize RTM results of three models and take difference of them to compare the locations where P-S wave generated. **Fig. 6** shows the differences between normalized RTM results of x-direction displacement; (a) is "isotropic model - 30% VTI model" and (b) is that of "isotropic model - 10% VTI model". **Fig. 6** shows differences of normalized RTM results in the depth up to z = 1000m beneath line B. In **Fig. 6**, white parts (large amplitude) are horizontally located around layer boundaries and **Fig. 6(a)** has stronger signal than **Fig. 6(b)**. These results mean that stronger VTI model has larger difference of location P-S converted wave generated comparing isotropic case.

(2) Proposed wave separation method

In this section, we use the new wave separation method mentioned in the section 2 to extract P-S wave from received waveforms for RTM. First, direct P-wave and S-wave are muted in received waveforms. Then, we use our wave separation method to divide P-S and S-P converted waves. **Fig. 7** shows displacement potentials in line B of 30% VTI model. **Fig. 8** shows SV-wave displacement calculated using potentials of **Fig. 7(c)**. In **Fig. 8**, we can see unignorable amplitude in arrival time of not only P-S wave but also S-P waves in x- and z-directions. **Fig. 9** shows orbits in vertical XZ plane calculated using SV-wave displacement of **Fig. 8** in several receiver points of line B. So that propagation direction of P-S and S-P waves is upper right, it can be said that orbits of **Fig. 9** behave like shear wave. Thus, we can say that signals in **Fig. 8** are identified as shear wave by the wave separation method.

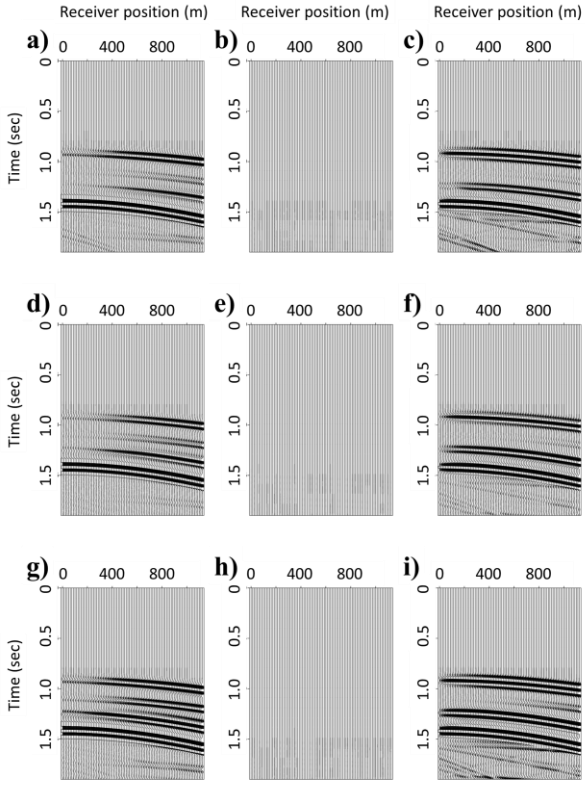

Figure 4 Received waveforms of displacement velocity on line B: (a), (b), (c) are 30% VTI model; (d), (e), (f) are 10% VTI model; (g), (h), (i) are isotropic model; and (a), (d), (g) are x-direction displacement velocity; (b), (e), (h) are y-direction; (c), (f), (i) are z-direction.

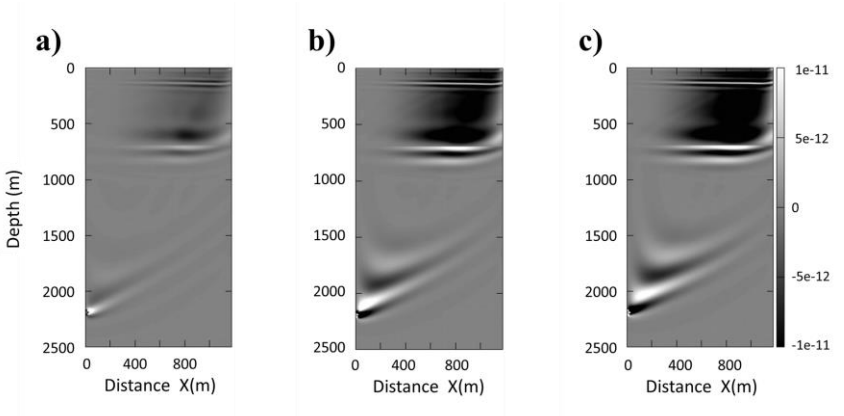

Figure 5 RTM results of x-direction displacement: (a) is 30% VTI model, (b) is 10% VTI model and (c) is isotropic model.

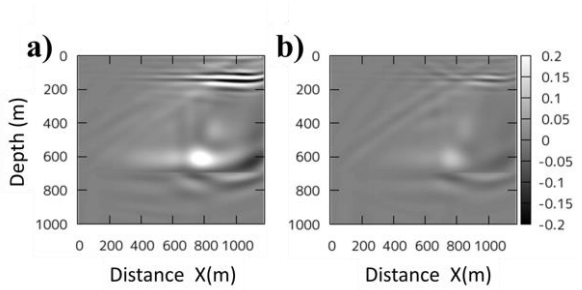

Figure 6 Differences of normalized RTM results in the depth up to z = 1000m beneath line B. (a) is "isotropic model – 30% VTI model" and (a) is "isotropic model – 10% VTI model".

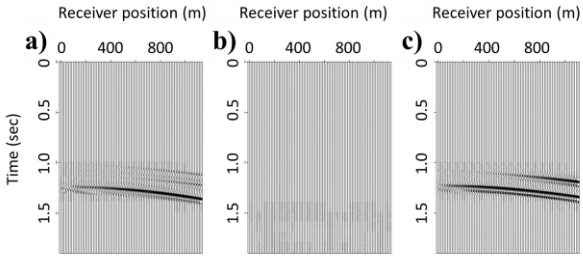

Figure 7 Displacement potentials of 30% VTI model in line B; (a) is P-wave potential ϕ, (b) is SH-wave potential χ, (c) is SV-wave potential ψ.

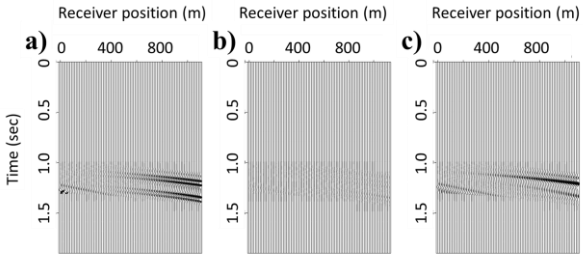

Figure 8 Displacement calculated using SV-wave potential ψ of 30% VTI model. (a), (b), (c) are x-, y-, z-direction displacement velocity, respectively.

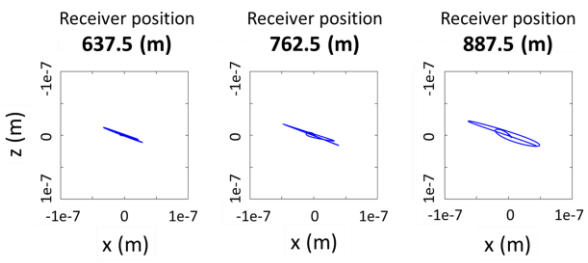

Figure 9 Orbits in vertical XZ plane calculated using SV-wave displacement of **Fig. 8** in the receiver points (a) 637.5m, (b) 762.5m and (c) 887.5m.

Next, we calculate RTM imaging results using SV-wave displacement calculated from potentials. **Fig. 10** are RTM results in vertical planes just beneath line B of 30% VTI model. We can see two strong signals around z = 700m and z = 1000m. The layer boundary in z = 678.5m is well detected as previous section, but the signal around z = 1000m is artifact noise which caused to recorded S-P wave extracted as shear wave by this wave separation method. Based on the above, although this wave separation method needs to be improved in the part of separating P and SV wave potentials, it has a possibility for obtaining information of subsurface strong anisotropy using RTM.

5. CONCLUSION

In this study, we focus on P-S converted wave that generated at boundary of anisotropic and isotropic media. We build a hypothesis that we could identify location of anisotropic material which affects received waveforms using RTM with P-S converted wave. Our numerical results show that there is important difference in location of strong signals and this important difference could be used for improving exploration method for strongly anisotropic media. Additionally, new wave separation method using displacement potentials still needs to be developed in separating P-wave potential and SV-wave potential, it has possibility to be used for imaging layer boundary between isotropic and anisotropic layers which generates PS converted waves.

REFERENCES

1) Sone, H., 2012, Mechanical properties of shale gas reservoir rocks and its relation to the in-situ stress variation in shale gas reservoir, *Ph.D. Thesis, Stanford University*, 225pp.
2) Thomsen, L., 1986, Weak elastic anisotropy, *Geophysics*, **51** (10), 1954-1966.
3) Yoneki, R., Mikada, H., Takekawa, J. 2016, Numerical study for anisotropic influences on elastic wavefields near surface. *The 20th International Symposium on Recent Advances in Exploration Geophysics (RAEG 2016) extended abstract*.
4) Claerbout, J. F., 1971, Toward a unifield theory of reflector mapping. *Geophysics* **36**(3), 467-481.
5) Saito, M., 2009, Jishin-Hado-ron. University of Tokyo Press, 122-138.
6) Aki, K. and Richards, P. G., 2002, Quantitative seismology, University Sience Book (transrated in Japanese by Uenishi, K., Kame, N., Aochi, H., 2004, Kokon-shoin)
7) Saenger, E. H., Gold, N., and Shapiro, S. A., 2000, Modeling the propagation of elastic waves using a modified fnite-difference grid, *Wave motion*, **31** (1), 77-92.
8) Komatitsch, D., Martin, R., 2007, An unsplit convolutional perfectly matched layer improved at grazing incidence for the seismic wave equation, *Geophysics*, **72**, 155-167.

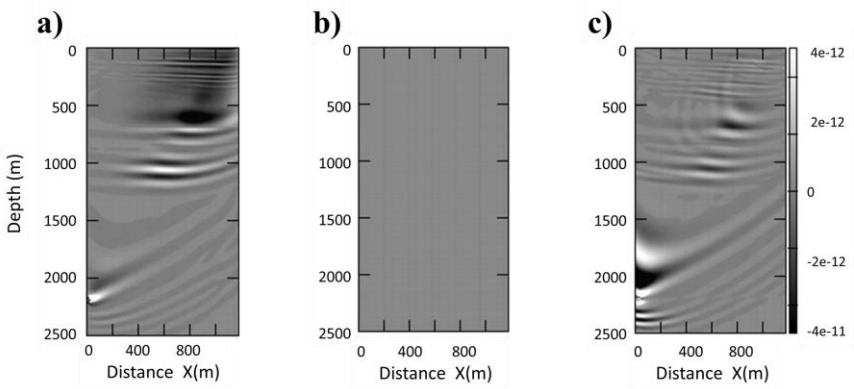

Figure 10 RTM imaging results of 30% VTI model calculated using SV-wave displacement in **Fig. 8**. (a), (b), (c) are results of x-, y-, z-direction displacement, respectively